



<b>Publication Year</b>	2018
<b>Acceptance in OA</b>	2021-04-27T14:28:05Z
<b>Title</b>	MAORY for ELT: preliminary design overview
<b>Authors</b>	CILIEGI, Paolo, DIOLAITI, EMILIANO, ABICCA, Renata, AGAPITO, GUIDO, Aliverti, Matteo, ARCIDIACONO, CARMELO, AURICCHIO, NATALIA, BALESTRA, Andrea, BARUFFOLO, Andrea, BELLAZZINI, Michele, BONAGLIA, MARCO, BREGOLI, Giovanni, Brissaud, Olivier, BUSONI, LORENZO, Carlotti, Alexis, CASCONI, Enrico, Correia, Jean-Jacques, CORTECCHIA, Fausto, Cosentino, Giuseppe, D'ORAZI, VALENTINA, DALL'ORA, Massimo, DE CAPRIO, VINCENZO, DE ROSA, ADRIANO GIUSEPPE, Delboulb�, Alain, DI ANTONIO, IVAN, DI RICO, Gianluca, DOLCI, Mauro, ESPOSITO, Simone, FANTINEL, Daniela, Feautrier, Philippe, FIORENTINO, Giuliana, FOPPIANI, ITALO, GIRO, Enrico, Gluck, Laurence, GRANI, PAOLO, GREGGIO, DAVIDE, H�nault, Fran�ois, Jocu, Laurent, La Penna, Paolo, Lafrasse, Sylvain, LAURIA, MIMMA, Le Coarer, Etienne, Le Louarn, Miska, LOMBINI, MATTEO, Magnard, Yves, MAGRIN, DEMETRIO, MAIORANO, Elisabetta, MANNUCCI, FILIPPO, Marchetti, Enrico, Maurel, Didier, Michaud, Laurence, Moraux, Estelle, MORGANTE, GIANLUCA, Moulin, Thibaut, Oberti, Sylvain, PARIANI, Giorgio, Patti, Mauro, PLANTET, CEDRIC ANTOINE ADRIEN GABRIEL, PODIO, LINDA, PUGLISI, Alfio Timothy, Rabou, Patrick, RAGAZZONI, Roberto, REDAELLI, EDOARDO MARIA ALBERTO, RIVA, Marco, Rochat, Sylvain, Roussel, Fr�d�ric, Roux, Alain, SALASNICH, Bernardo, SARACCO, Paolo, SCHREIBER, LAURA, SPAVONE, MARILENA, Stadler, Eric, Sztefek, Marie-H�l�ne, TEREZI, LUCA, VALENTINI, Angelo, Ventura, No�l., V�rinaud, Christophe, ZAGGIA, Simone
<b>Publisher's version (DOI)</b>	10.1117/12.2313672
<b>Handle</b>	<a href="http://hdl.handle.net/20.500.12386/30935">http://hdl.handle.net/20.500.12386/30935</a>
<b>Serie</b>	PROCEEDINGS OF SPIE
<b>Volume</b>	10703

# PROCEEDINGS OF SPIE

[SPIDigitalLibrary.org/conference-proceedings-of-spie](https://spiedigitallibrary.org/conference-proceedings-of-spie)

## MAORY for ELT: preliminary design overview

Cilieggi, Paolo, Diolaiti, Emiliano, Abicca, Renata, Agapito, Guido, Aliverti, Matteo, et al.

Paolo Cilieggi, Emiliano Diolaiti, Renata Abicca, Guido Agapito, Matteo Aliverti, Carmelo Arcidiacono, Natalia Auricchio, Andrea Balestra, Andrea Baruffolo, Michele Bellazzini, Marco Bonaglia, Giovanni Bregoli, Olivier Brissaud, Lorenzo Busoni, Alexis Carlotti, Enrico Cascone, Jean-Jacques Correia, Fausto Cortecchia, Giuseppe Cosentino, Valentina D'Orazi, Massimo Dall'Ora, Vincenzo De Caprio, Adriano De Rosa, Alain Delboulbé, Ivan Di Antonio, Gianluca Di Rico, Mauro Dolci, Simone Esposito, Daniela Fantinel, Philippe Feautrier, Giuliana Fiorentino, Italo Foppiani, Enrico Giro, Laurence Gluck, Paolo Grani, Davide Greggio, François Hénault, Laurent Jocou, Paolo La Penna, Sylvain Lafrasse, Mimma Lauria, Etienne Le Coarer, Miska Le Louarn, Matteo Lombini, Yves Magnard, Demetrio Magrin, Elisabetta Maiorano, Filippo Mannucci, Enrico Marchetti, Didier Maurel, Laurence Michaud, Estelle Moraux, Gianluca Morgante, Thibaut Moulin, Sylvain Oberti, Giorgio Pariani, Mauro Patti, Cedric Plantet, Linda Podio, Alfio Puglisi, Patrick Rabou, Roberto Ragazzoni, Edoardo Redaelli, Marco Riva, Sylvain Rochat, Frédéric Roussel, Alain Roux, Bernardo Salasnich, Paolo Saracco, Laura Schreiber, Marilena Spavone, Eric Stadler, Marie-Hélène Sztefek, Luca Terenzi, Angelo Valentini, Noël Ventura, Christophe Vérinaud, Simone Zaggia, "MAORY for ELT: preliminary design overview," Proc. SPIE 10703, Adaptive Optics Systems VI, 1070311 (18 July 2018); doi: 10.1117/12.2313672

**SPIE.**

Event: SPIE Astronomical Telescopes + Instrumentation, 2018, Austin, Texas, United States

# MAORY for ELT: preliminary design overview

Paolo Ciliegi\*<sup>a</sup>, Emiliano Diolaiti<sup>a</sup>, Renata Abicca<sup>a</sup>, Guido Agapito<sup>b</sup>, Matteo Aliverti<sup>c</sup>, Carmelo Arcidiacono<sup>a</sup>, Natalia Auricchio<sup>a</sup>, Andrea Balestra<sup>d</sup>, Andrea Baruffolo<sup>d</sup>, Michele Bellazzini<sup>a</sup>, Marco Bonaglia<sup>b</sup>, Giovanni Bregoli<sup>a</sup>, Olivier Brissaud<sup>e</sup>, Lorenzo Busoni<sup>b</sup>, Alexis Carlotti<sup>e</sup>, Enrico Cascone<sup>f</sup>, Jean-Jacques Correia<sup>e</sup>, Fausto Cortecchia<sup>a</sup>, Giuseppe Cosentino<sup>g</sup>, Valentina D'Orazi<sup>d</sup>, Massimo Dall'Ora<sup>f</sup>, Vincenzo De Caprio<sup>f</sup>, Adriano De Rosa<sup>a</sup>, Alain Delboulbé<sup>e</sup>, Ivan Di Antonio<sup>h</sup>, Gianluca Di Rico<sup>h</sup>, Mauro Dolci<sup>h</sup>, Simone Esposito<sup>b</sup>, Daniela Fantinel<sup>d</sup>, Philippe Feautrier<sup>e</sup>, Giuliana Fiorentino<sup>a</sup>, Italo Foppiani<sup>a</sup>, Enrico Giro<sup>d</sup>, Laurence Gluck<sup>e</sup>, Paolo Grani<sup>b</sup>, Davide Greggio<sup>d</sup>, François Hénault<sup>e</sup>, Laurent Jocou<sup>e</sup>, Paolo La Penna<sup>i</sup>, Sylvain Lafrasse<sup>e</sup>, Mimma Lauria<sup>b</sup>, Etienne Le Coarer<sup>e</sup>, Miska Le Louarn<sup>i</sup>, Matteo Lombini<sup>a</sup>, Yves Magnard<sup>e</sup>, Demetrio Magrin<sup>d</sup>, Elisabetta Maiorano<sup>a</sup>, Filippo Mannucci<sup>b</sup>, Enrico Marchetti<sup>i</sup>, Didier Maurel<sup>e</sup>, Laurence Michaud<sup>e</sup>, Estelle Moraux<sup>e</sup>, Gianluca Morgante<sup>a</sup>, Thibaut Moulin<sup>e</sup>, Sylvain Oberti<sup>i</sup>, Giorgio Pariani<sup>c</sup>, Mauro Patti<sup>a</sup>, Cedric Plantet<sup>b</sup>, Linda Podio<sup>b</sup>, Alfio Puglisi<sup>b</sup>, Patrick Rabou<sup>e</sup>, Roberto Ragazzoni<sup>d</sup>, Edoardo Redaelli<sup>c</sup>, Marco Riva<sup>c</sup>, Sylvain Rochat<sup>e</sup>, Frédéric Roussel<sup>e</sup>, Alain Roux<sup>e</sup>, Bernardo Salasnich<sup>d</sup>, Paolo Saracco<sup>c</sup>, Laura Schreiber<sup>a</sup>, Marilena Spavone<sup>f</sup>, Eric Stadler<sup>e</sup>, Marie-Hélène Sztefek<sup>e</sup>, Luca Terenzi<sup>a</sup>, Angelo Valentini<sup>h</sup>, Noël Ventura<sup>e</sup>, Christophe Vérinaud<sup>i</sup>, Simone Zaggia<sup>d</sup>

<sup>a</sup>INAF – Osservatorio di Astrofisica e Scienza dello Spazio di Bologna,  
via Gobetti 93/3, 40129 Bologna, Italy;

<sup>b</sup>INAF – Osservatorio Astrofisico di Arcetri, largo E. Fermi 5, 50125 Firenze, Italy;

<sup>c</sup>INAF – Osservatorio Astronomico di Brera, via E. Bianchi 46, 23807 Merate, Italy;

<sup>d</sup>INAF – Osservatorio Astronomico di Padova, vicolo dell'Osservatorio 5, 35122 Padova, Italy;

<sup>e</sup>INSU – IPAG, 414 rue de la piscine, BP 53, 38041 Grenoble Cedex 9, France;

<sup>f</sup>INAF – Osservatorio Astronomico di Capodimonte, Salita Moiariello 16, 80131 Napoli, Italy;

<sup>g</sup>Università di Bologna – DIFA, via Gobetti 93/3, 40129 Bologna, Italy;

<sup>h</sup>INAF – Osservatorio Astronomico d'Abruzzo, via Maggini snc, 64100 Teramo, Italy;

<sup>i</sup>European Southern Observatory, K.-Schwarzschild-Str. 2, 85748 Garching b. Muenchen, Germany;

## ABSTRACT

MAORY is one of the approved instruments for the European Extremely Large Telescope. It is an adaptive optics module, enabling high-angular resolution observations in the near infrared by real-time compensation of the wavefront distortions due to atmospheric turbulence and other disturbances such as wind action on the telescope. An overview of the instrument design is given in this paper.

**Keywords:** Extremely Large Telescopes, ELT, Multi-Conjugate Adaptive Optics, Laser Guide Stars, Sky Coverage

## 1. INTRODUCTION

The MAORY<sup>[1]</sup> adaptive optics module for the European Extremely Large Telescope (ELT)<sup>[2][3]</sup> is designed to support the MICADO<sup>[4]</sup> near-infrared camera by offering two adaptive optics modes: Multi-Conjugate Adaptive Optics (MCAO) and Single-Conjugate Adaptive Optics (SCAO). MAORY also offers provision for a second port for a future instrument, as yet undefined. The project is progressing in its phase B towards the Preliminary Design Review. An overview of the current design and expected performance is given in this paper.

\*paolo.ciliegi@oabo.inaf.it; phone +39 051 6357312; fax +39 051 6357390; www.oabo.inaf.it

The MCAO mode of MAORY achieves spatially uniform adaptive optics compensation over the scientific field of view with high sky coverage; wavefront sensing is performed by up to six artificial Laser Guide Stars (LGS) and up to three Natural Guide Stars (NGS), respectively for the measurement of high and low-order wavefront perturbations; wavefront compensation is performed by adaptive Deformable Mirrors (DMs) in MAORY, which work together with the telescope's adaptive and tip-tilt mirrors M4 and M5 respectively.

The SCAO mode achieves peak adaptive optics performance on a limited field of view, when a sufficiently bright reference object is available nearby the scientific target; wavefront distortions are measured by a single NGS wavefront sensor and compensated by the telescope M4 and M5 mirrors, while the adaptive mirrors inside MAORY are kept fixed at their reference shape. The development of the SCAO mode is a joint endeavour between the MAORY and MICADO instrument teams<sup>[5]</sup>.

From the opto-mechanical point of view, MAORY consists of an optical relay, which re-images the telescope focal plane for the science instruments. The relay is supported by an optical bench, which is mounted on the telescope Nasmyth platform in gravity invariant configuration. The relay consists of six mirrors and a dichroic beam-splitter, which separates the science light from the LGS light. The relatively low number of optical elements is a design choice to reduce thermal background from the optics, which work at ambient temperature. MAORY has to provide up to two DMs in the optical relay, one DM being the minimum to perform MCAO correction in conjunction with the telescope's M4 and M5. The DMs are the third and fourth mirrors in the relay and are optically conjugated to about 15 km and 4 km from the telescope entrance pupil. The DM conjugated to lower range may be replaced by a rigid mirror in a single post-focal DM implementation of MAORY.

The light of the six LGSs, which are launched from the edge of the telescope aperture fixed with respect to the telescope pupil, is focused by an LGS objective. The LGS images produced by this objective are selected by pick-off mirrors, which feed the six probes of the LGS wavefront sensor. The LGSs are launched 45 arcsec off-axis, as a baseline for the MICADO application. Larger angles are possible to ensure uniform compensation for a wide-field instrument on the second exit port. The LGS wavefront sensor consists of 6 Shack-Hartmann wavefront sensors of order 80x80 sub-apertures.

At the exit focal plane of the MAORY optical relay, the light of up to three NGSs over a patrol field of view of 180 arcseconds angular diameter is selected by three pick-off mirrors and fed into the NGS wavefront sensor module. Each NGS wavefront sensor probe consists of two channels: the Low-Order WFS channel, including a 2x2 Shack-Hartmann WFS working in the wavelength range 1.5-1.8  $\mu\text{m}$  at adaptive optics speed, and the Reference WFS channel, including a 10x10 Shack-Hartmann WFS working in the wavelength range 0.6-1.0  $\mu\text{m}$  at slow speed, with the function of detrending the LGS wavefront sensor measurements from spurious effects associated to the sodium layer features.

The MAORY real-time computer collects the signals from all wavefront sensing channels and computes the commands for the post-focal adaptive DMs and for the telescope M4 and M5 mirrors. The baseline wavefront reconstruction approach is Pseudo-Open Loop Control.

MAORY is required to deliver a Strehl ratio of 0.3 (goal 0.5) at 2.2  $\mu\text{m}$  wavelength over a field of view of 1 arcminute. This performance has to be achieved with 50% sky coverage across the whole sky.

## 2. INSTRUMENT ADAPTIVE OPTICS ARCHITECTURE

### 2.1 Wavefront control interface with the adaptive telescope

Wavefront control is based on distributed resources in the telescope and in MAORY. The control equipment of the adaptive ELT maintains the telescope alignment at a level such that the optical quality is within the capture range of MAORY. Quasi-static aberrations in the telescope are compensated by the active optics system. Adaptive optics compensation of fast wavefront aberrations due to atmospheric turbulence, windshake effects etc. relies on resources distributed in MAORY (LGS and NGS wavefront sensors, post-focal DMs, real-time computer) and in the telescope (LGS launchers, adaptive quaternary mirror M4, tip-tilt mirror M5, other actuators such as the telescope main structure).

### 2.2 MCAO mode

The instrument sub-systems and their inter-relations in MCAO mode are shown in the functional block diagram in Figure 1, which also shows the different light paths in the instrument and the control signal flow. The MCAO mode of MAORY is based on the use of six LGS Wavefront Sensors (WFS) and up to three NGS wavefront sensors.

The light from the telescope, already pre-compensated by the actuators in the telescope, is propagated through the MAORY main path optics (common path). Upon wavefront compensation by the post-focal DMs (INS-DM1 and INS-DM2 in the picture), the light is split by a dichroic beam-splitter.

The light of wavelength shorter than about 600 nm is propagated from the dichroic beam-splitter to the LGS path optics (also known as LGS objective) and then to the LGS wavefront sensor sub-system (WFS-LGS in the picture). The light of wavelength longer than about 600 nm is propagated from the dichroic beam-splitter through the last segment of the main path optics (science path) to the exit port.

At the exit port, the MAORY focal plane is made available to MICADO, or another instrument in the case of the second port. The light of the NGSs is picked off by the Low-Order and Reference (LOR) wavefront sensor units in the NGS wavefront sensor module<sup>[5]</sup>. The LOR wavefront sensor serves different functions, among which: i) measuring the low-order modes (tip-tilt, but also focus and astigmatism) which are not reliably measured by the LGS wavefront sensor, due to the well-known tilt indetermination problem and to fast sodium layer instabilities (WFS-NGS-LO channel in the picture); ii) providing a way to “de-trend” the low/medium order modes, other than tip-tilt, focus and astigmatism, which are affected by sodium layer temporal variations coupled to instrumental effects in the LGS wavefront sensor such as spot truncation<sup>[6]</sup> (WFS-NGS-Ref in the picture).

The wavefront measurements performed by the LGS and LOR wavefront sensors are processed by the MAORY Real Time Computer (INS-RTC in the picture), which drives in closed loop the post-focal DMs and, through the telescope Centralised Control System (CCS), also the actuators in the telescope, including the adaptive quaternary mirror M4 and the tip-tilt mirror M5.

All instrument operations are controlled and supervised by the MAORY Instrument Control System (ICS) software, which also provides interfaces to the telescope CCS and to the MICADO (or other) client instrument ICS software.

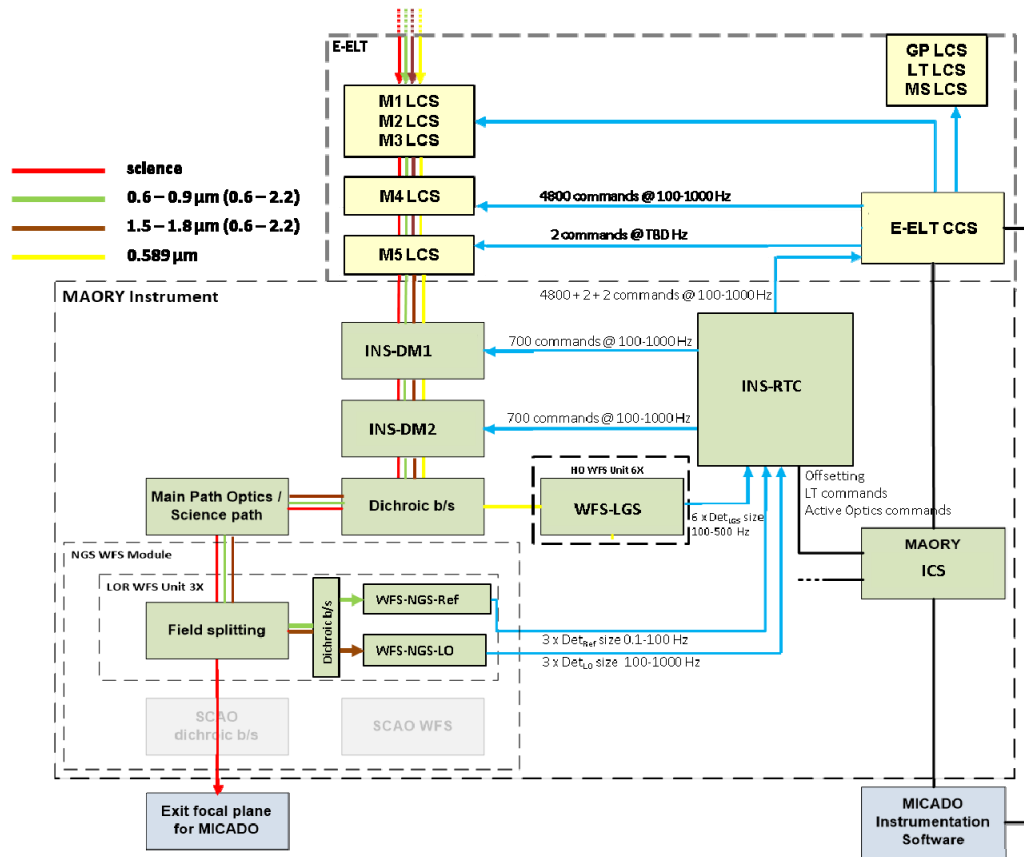


Figure 1. MCAO functional block diagram. Colour codes for the light beam according to wavelength are shown in the upper left part of the figure. Blue lines represent real-time signals. Black lines represent non real-time signals. Light grey blocks are not used in MCAO mode.

### 2.3 SCAO mode

In the SCAO mode the LGS and the LOR wavefront sensors are not used. A dedicated SCAO wavefront sensor is used instead.

The light path is essentially the same as in the MCAO mode, with the exception of the exit port. Here the light of a NGS nearby the scientific target of interest is selected in wavelength by a deployable SCAO dichroic beam-splitter, which is inserted in the beam just upstream the exit focal plane. This SCAO dichroic beam-splitter transmits the science wavelengths to MICADO and reflects the wavefront sensing wavelengths to the SCAO wavefront sensor.

Signals from the SCAO wavefront sensor in the NGS wavefront sensor module are read by the MAORY RTC, which drives the actuators in the telescope through the CCS.

In the SCAO mode the MAORY post-focal DMs are kept at their reference shape as a baseline.

## 3. INSTRUMENT DESIGN AND EXPECTED PERFORMANCE

### 3.1 Post-focal relay optics and main structure

The post-focal relay optics sub-system of MAORY<sup>[7]</sup> re-images the telescope focal plane to the exit ports. The layout of the post-focal relay optics is shown in Figure 2.

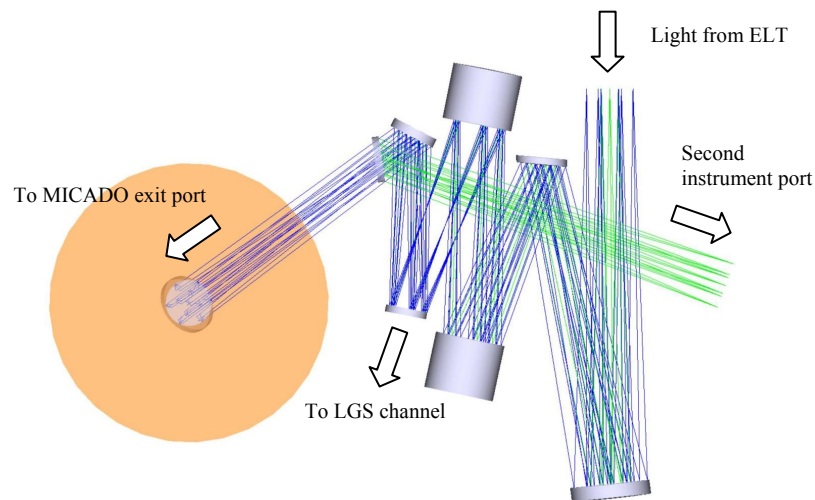


Figure 2. Post-focal relay optical layout. Only the science path is shown for simplicity. Blue rays: light path to MICADO port; green rays: light path to second instrument port (achieved by deployable flat mirror). The orange circle represents the approximate volume of MICADO.

The sub-system contains the following channels:

- main path optics, which relay the telescope focal plane to the exit ports for the science instruments (MICADO and second instrument as yet undefined);
- LGS objective, which creates an image plane for the LGS wavefront sensor sub-system.

Light separation between the two channels is accomplished by the LGS dichroic beam-splitter, which splits the light according to wavelengths.

Inside the optical path, two clear planes are created, optically conjugated to two different ranges from the telescope entrance pupil, allowing the insertion of up to two DMs.

The main path optics design is based on six mirrors and the above mentioned LGS dichroic beam-splitter. In the baseline configuration, the beam-splitter is assumed to reflect the science path wavelengths: in this way, the path from the telescope focal plane to the instrument focal plane consists of reflecting optics only, nominally free from chromatic effects. The number of mirrors has been minimised to reduce thermal emissivity, as MAORY is not cooled as a baseline:

the thermal background is therefore controlled by minimum number of optics and by suitable maintenance procedures to ensure optics cleanliness. Two mirrors are adaptive in the full instrument configuration; a partial implementation with one DM only is possible, with the second DM replaced by a rigid mirror.

The LGS objective design is based on both mirrors and lenses. The exit focal ratio is F/5, to reduce the focus range when the sodium layer distance changes with zenith distance during observations. The exit pupil is at infinity, in order to keep the pupil image size constant inside the wavefront sensor.

The main parameters of the main path optics and of the LGS objective are reported in the next tables.

Table 1. Main path optics parameters.

Item	Value
Exit focal ratio	F/17.7 (1:1 relay)
NGS patrol FoV (also called technical FoV)	180 arcsec diameter
MICADO science FoV	Up to 75 arcsec diameter
Transmitted wavelength range at exit port	0.6 – 2.5 $\mu\text{m}$ Lower wavelength limit set by LGS dichroic
Post-focal DMs conjugation range	15 km, 4 km
Projected actuator pitch of DMs on conjugates	$\sim 1.5$ m

Table 2. LGS objective parameters.

Item	Value
Operating wavelength	0.589 $\mu\text{m}$
LGS range to be re-imaged	84 – 240 km
Exit focal ratio	F/5
LGS constellation angular diameter	90 – 120 arcsec

The exit port for MICADO is gravity invariant. The exit port for the second instrument is created by inserting a deployable flat mirror in the optical path; this port is not gravity-invariant.

The mechanical layout of the instrument<sup>[8]</sup> is shown in Figure 3. The post-focal relay optics is supported by the instrument main structure, which consists of a bench, connected to the Nasmyth platform through a support system made of four bipods in the current design, and a cover, which is aimed at creating an isothermal environment around the optics.

A passive thermal concept is adopted. Daytime ventilation of the optics is planned, to help thermalisation by flushing cold air at the foreseen temperature for the night. During night-time, MAORY follows the ambient temperature.

MICADO is detached from MAORY and is supported by its own support system. Active and adaptive compensation of relative instabilities between the two instruments will be needed: in particular, any relative tip-tilt measurement between MAORY and MICADO is ensured by the MAORY LOR wavefront sensor (section 3.3), which is mounted directly on MICADO.

The last mirror of the MAORY main path optics is flat and folds the light down to MICADO in gravity invariant configuration. M11 is supported by tripod system, which is connected to the MICADO fixed structure.

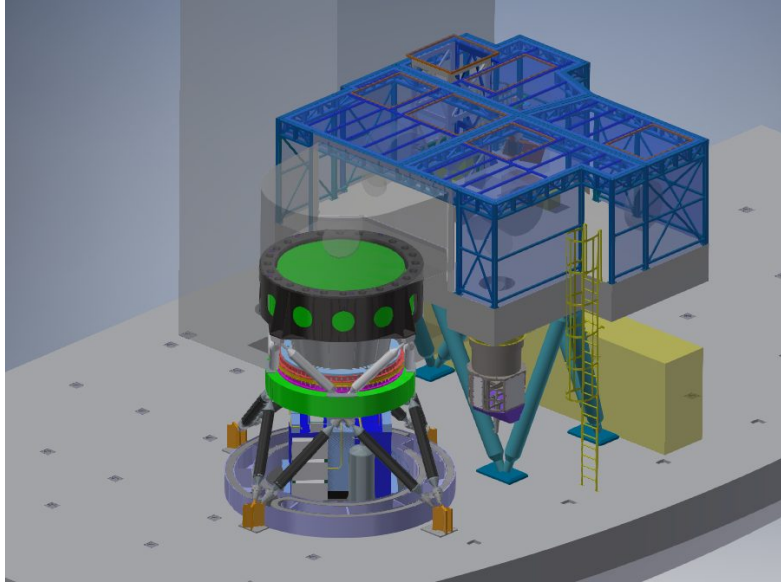


Figure 3. MAORY mechanical layout on the ELT Nasmyth platform. MICADO is also shown on the foreground.

### 3.2 LGS wavefront sensor

The opto-mechanical layout of the LGS wavefront sensor<sup>[9]</sup> is shown in Figure 4. The sub-system is attached to the bottom plane of the MAORY bench in gravity-invariant configuration, to ensure stable mounting.

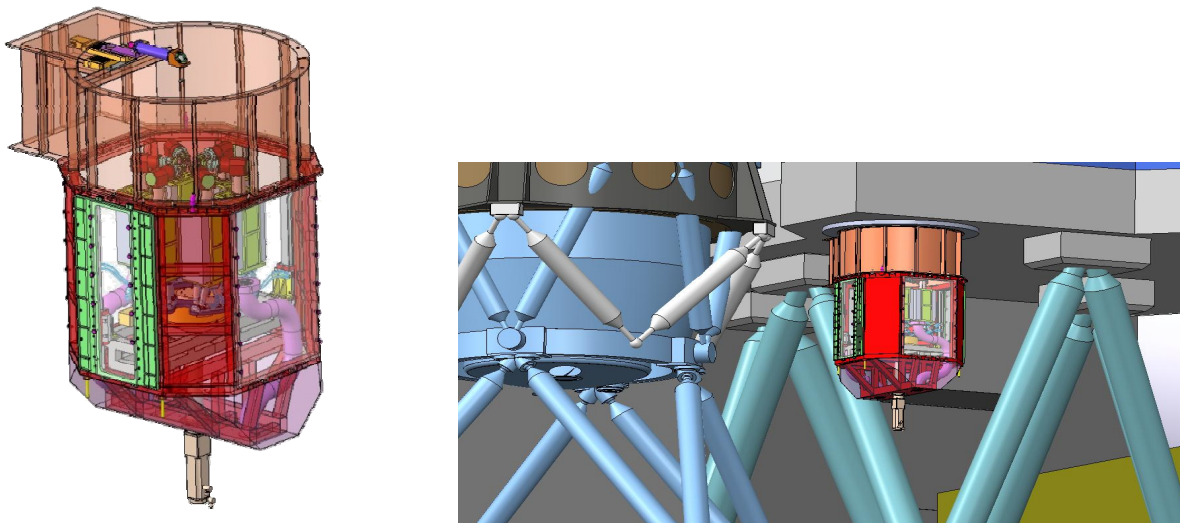


Figure 4. Left: LGS wavefront sensor opto-mechanical assembly. Right: the sub-system is attached to the bottom of the MAORY bench in gravity invariant configuration.

The LGS wavefront sensor consists of six WFS probes, one per LGS. The probes are mounted on a common focusing stage, to track the global sodium focus as the zenith angle changes during the observation, and on a common rotation stage, to track the rotation of the LGS asterism with the elevation axis, as the LGSs are launched fixed with respect to the telescope pupil. Each wavefront sensor probe is also provided with its own hexapod system for differential adjustments.

The images of the LGSs, produced by the LGS objective described in section 3.1, are selected by pick-off mirrors, which feed the six LGS wavefront sensor probes. The LGSs are launched 45 arcsec off-axis, as a baseline for the MICADO

application. Larger angles are possible to ensure uniform compensation for a wide-field instrument on the second exit port.

The LGS jitter compensation function, which was previously implemented also inside each LGS probe, is now implemented by the LGS launchers in the telescope.

The LGS wavefront sensor is based on a Shack-Hartmann configuration of order  $80 \times 80$  sub-apertures. The baseline detector choice allows  $10 \times 10$  pixels per subaperture. A trade-off study is in progress regarding the field of view and the spot sampling. Possible choices are 15 arcsec field of view with 1.5 arcsec/pixel sampling or 10 arcsec field of view with 1 arcsec/pixel sampling. The former reduces LGS spot truncation effects, relaxing the requirements on the NGS Reference wavefront sensor; the latter is better in terms of spot sampling. Mitigation strategies are under study to control the issues which are present in both cases. In particular, mitigation strategies for under-sampling effects are LGS spot blurring, if the LGS flux is high enough to preserve measurement sensitivity, and wavefront sensor response calibration techniques by spot modulation. Mitigation strategies for spot truncation are the use of advanced tomographic schemes, weighting the slope measurements according to the elongation of the corresponding spots, and the use of advanced centroiding algorithms, such as matched filtering.

### 3.3 NGS wavefront sensor module

The NGS wavefront sensor module<sup>[10]</sup> is connected to the MICADO cryostat, in order to minimise non-common path aberrations with the science instrument, in particular differential tip-tilt.

The NGS wavefront sensor module is divided in two parts:

- LOR wavefront sensor plate, holding the three wavefront sensor probes for the MCAO mode;
- SCAO wavefront sensor plate, holding the wavefront sensor and other tools for the SCAO mode; the description of the SCAO wavefront sensor plate is beyond the scope of this paper.

The three probes of the LOR wavefront sensor for the MCAO mode cover a patrol field of view of up to 180 arcsec diameter. Each probe covers approximately 1/3 of the patrol field, with overlap.

Each LOR wavefront sensor probe is divided in two channels:

- Low-Order wavefront sensor channel, including a  $2 \times 2$  Shack-Hartmann wavefront sensor working in the 1.5-1.8  $\mu\text{m}$  wavelength range;
- Reference wavefront sensor channel, including a  $10 \times 10$  Shack-Hartmann wavefront sensor working in the 0.6-1.0  $\mu\text{m}$  wavelength range.

The Low-Order wavefront sensor channel measures tip-tilt, focus and astigmatism at adaptive optics speed. The Reference wavefront sensor channel operates at slow speed and is used to de-trend the measurements of the LGS wavefront sensor.

### 3.4 Real time control system

The MAORY RTC architecture<sup>[11]</sup> and the main control loops are shown in Figure 5.

The sensors are shown on the left: from top to bottom, these are the LGS wavefront sensor, the NGS Low-Order wavefront sensor and the NGS Reference wavefront sensor. The actuators are shown on the right: from bottom to top, these are the telescope's M4 and M5 (plus other actuators which are not shown here for simplicity), the MAORY post-focal DMs (called DM1 and DM2 in the diagram) and the LGS jitter compensation mirrors (JM), which are included in the LGS launch telescopes.

The LGS wavefront sensor images are calibrated and processed and the slopes are computed and filtered from tip-tilt, focus and astigmatism contributions. The tip-tilt signal is used to drive the LGS jitter compensation loop, which is shown in the upper part of the diagram, while the focus signal is used as an error signal to drive the focus compensation in the LGS wavefront sensor (this loop is not shown in the diagram). The filtered slopes are fed into the global tomographic reconstructor. In the simplest approach, the reconstructor is based on a Matrix-Vector-Multiply (MVM), where the control matrix is computed as pseudo-inverse of the WFSs-to-DMs interaction matrix, e.g. by truncated singular value decomposition. Also a more advanced POLC reconstructor<sup>[12]</sup> is considered, which is the current baseline. The baseline frame rate of the LGS wavefront sensor high-order loop is 500 Hz.

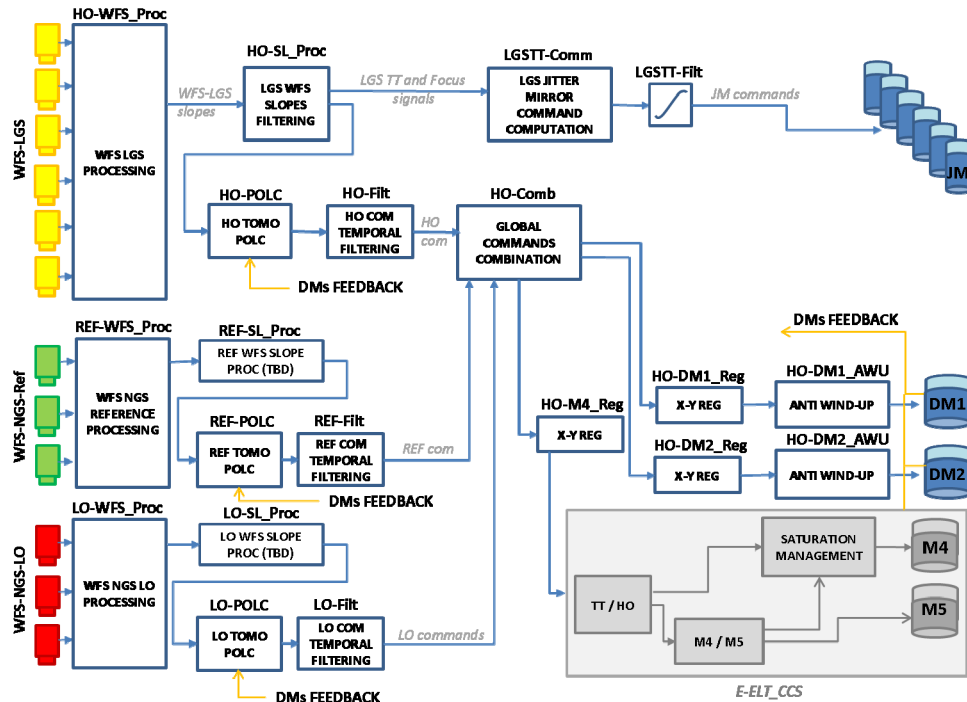


Figure 5. Real time control system architecture.

The NGS Reference wavefront sensor images are calibrated and processed and the slopes are computed and fed into the global tomographic reconstructor, to provide slope offsets for the LGS wavefront sensor slopes. The frame rate of the NGS Reference wavefront sensor loop is slow, typically 0.1-100 Hz.

The NGS Low-Order wavefront sensor images are calibrated and processed and the slopes (corresponding to the tip-tilt, focus and astigmatism modes) are fed into the global tomographic reconstructor. The frame rate of the NGS Low-Order wavefront sensor loop ranges from a minimum of 100 Hz to a maximum of 1000 Hz, also depending on the NGS brightness. The frame rate may be asynchronous on the three NGSs.

The commands produced by the tomographic reconstructor are temporally filtered and sent to the DMs. In the case of M4/M5, the commands are sent to the telescope CCS, which takes care of tip-tilt / high-order splitting between the actuators in the telescope.

### 3.5 MCAO performance

The optimisation of the MCAO architecture and the related performance estimation are carried by end-to-end simulation tools<sup>[13][14]</sup>.

In MCAO mode, MAORY will have to provide Strehl Ratio  $SR \geq 0.3$  at wavelength  $\lambda = 2.2 \mu\text{m}$  under median atmospheric conditions ( $r_0 = 0.157$  at  $\lambda = 0.5 \mu\text{m}$  wavelength). This requirement is intended as average value over the MICADO field of view for observations as close to zenith as allowed by the telescope. The requirement has to be achieved over at least 50% of the sky observable by the telescope, at any Galactic latitude. The performance goal, for the same conditions, is  $SR = 0.5$ .

Different system configurations are under investigation in the framework of the project phase B:

- 1 post-focal DM, with  $\sim 1.5$  m projected spacing;
- 2 post-focal DMs, with  $\sim 1.5$  m projected spacing;
- 1 post-focal DM, with  $\sim 0.5$  m projected spacing;

- Possible use of Dual Adaptive Optics<sup>[15]</sup>, consisting of dedicated DMs in the NGS Low-Order wavefront sensor channels, controlling about 100 modes in open loop, in order to shrink the NGS images, allowing the use of fainter NGS, thus increasing sky coverage.

A comparison of all these configurations is shown in Figure 6 for the reference median Cn2 profile. The figure shows the sky coverage as a function of Strehl Ratio on the MICADO field of view, considering NGS magnitude  $H < 22$  and allowing for 1, 2 or 3 NGS asterisms. All configurations give very similar performance. In particular, the 50% sky coverage is achieved with Strehl Ratio  $SR > 0.4$  at  $2.2 \mu\text{m}$  wavelength. From the preliminary results shown here, one might conclude that the simplest system configuration, with 1 post-focal DM only, is enough to achieve the required performance. However, at the moment of this writing, extensive analysis is in progress, in order to confirm this trend or to possibly find applications in which performance might significantly benefit from a second post-focal DM and/or from the implementation of a Dual Adaptive Optics approach. The current directions of investigation are: i) restricting the NGS limiting magnitude to  $H < 20$ , in order to maximise the probability of retrieving NGSs from star catalogues; ii) using 3-NGS asterisms only, in order to ensure better control of low-order modes, which may be affected by currently unknown effects, such as anisotropies in the sodium layer properties; iii) testing different Cn2 profiles, including samples with significantly more turbulence power in altitude than the reference profile.

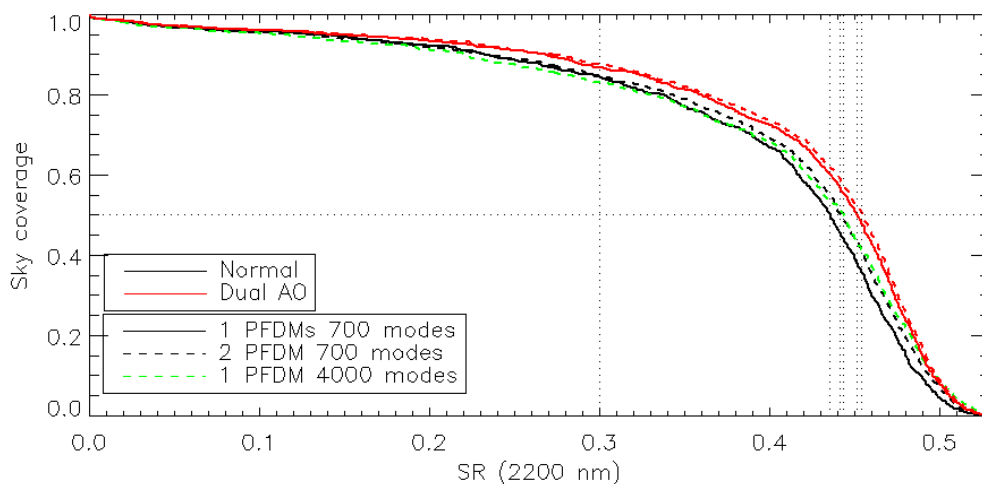


Figure 6. Sky coverage vs. Strehl Ratio at  $2.2 \mu\text{m}$  wavelength for different instrument configurations.

## ACKNOWLEDGMENTS

The MAORY instrument is developed in the framework of the Agreement No. 65221/ESO/15/67001/JSC between the European Organisation for Astronomical Research in the Southern Hemisphere (ESO) and the Istituto Nazionale di Astrofisica (INAF) on behalf of the Consortium consisting of INAF and of the Institut National des Sciences de l'Univers du Centre National de la Recherche Scientifique (INSU/CNRS) acting on behalf of the Institut de Planetologie et d'Astrophysique de Grenoble (IPAG).

This work has been partly supported by "Progetto Premiale E-ELT" funded by the Italian Ministry for Education, University and Research (MIUR).

## REFERENCES

- [1] Diolaiti, E., Ciliegi, P., Abicca, R., Agapito, G., et al., "MAORY adaptive optics module for the E-ELT," Proceedings of the SPIE 9909, article id. 99092D 7 pp. (2016).
- [2] Tamai, R., Cerasuolo, M., Gonzalez, J. C., Koehler, B., et al., "The E-ELT program status," Proceedings of the SPIE 9906, id. 99060W 13 pp. (2016).

- [3] Ramsay, S., Casali, M., Cirasuolo, M., Egner, S., et al., "Progress along the E-ELT instrumentation roadmap," Proceedings of the SPIE 9908, id. 99081T 12 pp. (2016).
- [4] Davies, R., Schubert, J., Hartl, M., Alves, J., et al., "MICADO: first light imager for the E-ELT," Proceedings of the SPIE 9908, id. 99081Z 12 pp. (2016).
- [5] Clénet, Y., et al., "MICADO-MAORY SCAO: towards the preliminary design review," this Conference.
- [6] Schreiber, L., Diolaiti, E., Arcidiacono, C., Pfrommer, T., Holzlöhner, R., Lombini, M., Hickson, P., "Impact of sodium layer variations on the performance of the E-ELT MCAO module," Proceedings of the SPIE 9148, id. 91486Q (2014).
- [7] Lombini, M., et al., "Optical design of the post focal relay of MAORY," Proceedings of the SPIE, Volume 10690, in press.
- [8] De Caprio, V., et al., "MAORY for ELT: preliminary mechanical design of the support structure," this Conference.
- [9] Schreiber, L., et al., "The MAORY laser guide star wavefront sensor: design status," this Conference.
- [10] Bonaglia, M., et al., "Status of the preliminary design of the NGS WFS subsystem of MAORY," this Conference.
- [11] Foppiani, I., et al., "MAORY real time computer preliminary design," this Conference.
- [12] Ellerbroek, B., Vogel, C. R., "Simulations of closed-loop wavefront reconstruction for multi-conjugate adaptive optics on giant telescopes," Proceedings of the SPIE 9909, Volume 5169, pp. 206-217 (2003).
- [13] Plantet, C., et al., "Performance analysis of the NGS WFS of MAORY," this Conference.
- [14] Arcidiacono, C., et al., "Numerical simulations of MAORY MCAO module for the ELT," this Conference.
- [15] Rigaut, F., Gendron, E., "Laser guide star in adaptive optics - The tilt determination problem," Astronomy and Astrophysics, Volume 261, pp. 677-684 (1992).